Magnetic Imaging through Metallic Enclosures

Brendan J. Darrer[1], Joe C. Watson[2], Paul Bartlett[1], Ferruccio Renzoni[1]

[1]Department of Physics & Astronomy, University College London, Gower Street, London, WC1E 6BT, United Kingdom

[2]Novel Detection Concepts, National Nuclear Security Programme, Atomic Weapons Establishment, Aldermaston, Reading, RG7 4PR, United Kingdom

Email: brendan.darrer.12@ucl.ac.uk

ABSTRACT

Security applications may require the ability to image through electromagnetic shields. This is for example the case when trafficking of illicit material involves cargo containers. Thus, suitable detection techniques are required to penetrate a ferromagnetic enclosure. We report on the demonstration of the ability of a system based on electromagnetic interrogation techniques to create magnetic images of metallic objects concealed within metallic enclosures. The penetrating power through single and double ferromagnetic enclosures was investigated. The instrument employs a driver Helmholtz-coil assembly and an array of 20 × 20 sensor coils. The sample objects were imaged via phase variation measurements between the driver and sensor coils, due to inductive coupling between the coils and the sample object.

Keywords Magnetic induction tomography (MIT), eddy currents, imaging, security.

1 INTRODUCTION

In this paper we consider the problem of electromagnetic imaging through metallic enclosures, as of interest in security applications. It is normally assumed that a ferromagnetic enclosure will act as a Faraday cage, and therefore screen any electromagnetic waves from penetrating, denying detection of any hidden metallic objects. However, imaging through metallic enclosures was demonstrated for the specific case of 50 μm thickness of copper pipe (Ma 2006). Here we report on imaging through a double enclosure of plated-mild-steel, with 0.24 mm and 0.33 mm thickness. This demonstrates that it is in fact possible to penetrate through such a thick enclosure assembly to image a concealed conductive-object, as illustrated in figure 1. Our experiments therefore validate electromagnetic detection as a potential imaging-technique for the security industry (see Darrer 2015a for a detailed discussion of security implications).

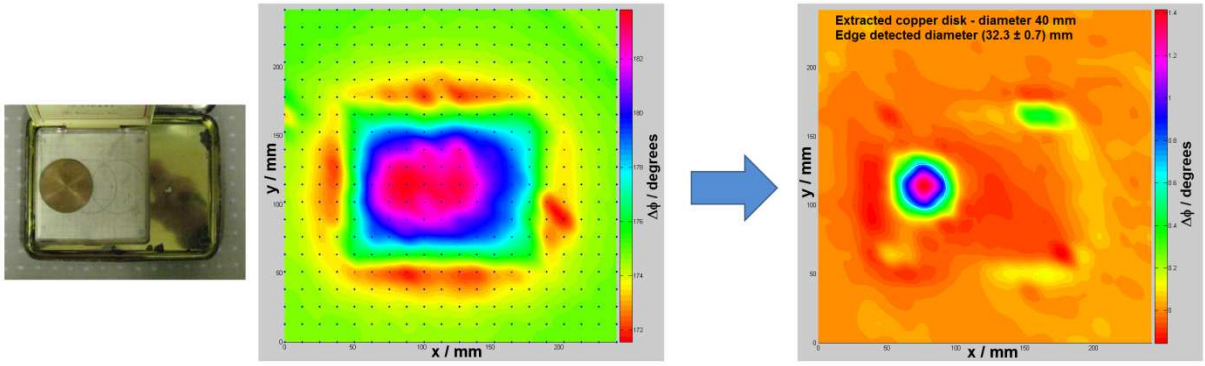

Figure 1: Magnetic image of copper disk, 40 mm diameter by 3 mm height, extracted from a double ferromagnetic enclosure.

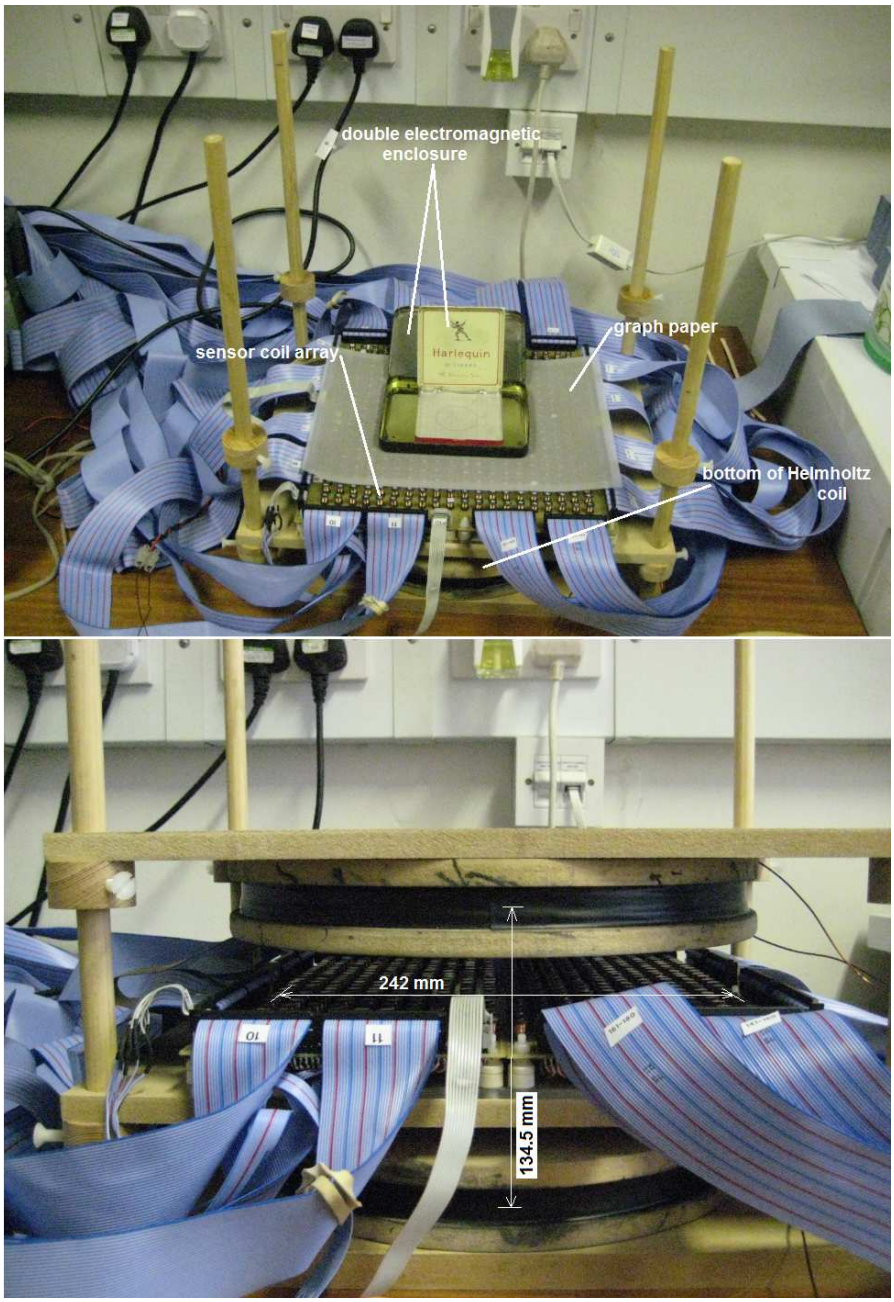

Figure 2: Helmholtz-coil assembly, with top coil removed, showing double-ferromagnetic enclosure resting on the sensor-coil array (Top). Side view of the Helmholtz coils and sensor-coil array (Bottom).

2 PRINCIPLE OF MAGNETIC IMAGING

Our magnetic-imaging system relies on the principles of electromagnetic induction and is a magnetic-induction-tomography (MIT) technique (Darrer 2015a; Griffiths 2001; Korjenevsky 2000). Firstly, a primary magnetic field induces eddy currents into the conductive sample-object, due to Faraday's law of induction. The eddy currents in turn generate a secondary-opposing field. The amplitude and phase of the total magnetic field, the sum of the eddy-current field and primary field, is measured after transmission through the metallic specimen. The measurement of amplitude and phase of the field translates as the potential-difference induced across the sensor coils. If the primary field is **B** and the secondary field is Δ**B**, the phase measurements between the voltage-signals of the driver and sensor coils are representative of the phase between **B** and Δ**B** + **B** due to Faraday's law induction **(**Griffiths 2001; Griffiths 2007). MIT is sensitive to all three passive electromagnetic properties of the specimen. These are conductivity, permeability and permittivity, with the ability of reconstructing images in the first two of these property-mediums and possibly the third, as reported by other researchers (Soleimani 2009). Positional-phase measurements allow reconstruction of the image by way of a 20 × 20 planar-sensor-coil array of dimensions 242 mm × 242 mm (Darrer 2015b; Ma 2013). The sensor coils are commercially available ferrite-cored inductors, each of 680 μH. Our planar arrangement of the sensor coils allows us to reconstruct images, without needing to solve the time consuming 'inverse problem', often implemented in MIT systems, due to their different coil-geometries. A more detailed description of our set-up can be found in (Darrer 2015b).

A measurement is made at each sensor-coil position of the time-varying magnetic field, consisting of the sum of the primary and secondary fields. This measurement is made in terms of the voltage induced in the coils. The voltage across each coil is measured from a dual-phase lock-in amplifier at frequencies of 200 Hz, 2 kHz and 10 kHz. This instrument has the capability of measuring voltage magnitude and phase-difference (phase) between signals in the driver and sensor coils, given as ϕ. The driving (primary) field is provided by the Helmholtz-coil assembly as shown in figure 2. Measurements of the phase-difference were taken at the centre point, (x, y), of each sensor-coil position. By cubic piecewise interpolation of the phase data (z axis) and positional data (x, y axes), a magnetic image can be constructed. To generate an image, firstly the background phase values, $\phi_0(x, y)$, are measured with no object present, and then one is made in the presence of the object, $\phi(x, y)$. The resultant magnetic image is the difference of the two phase-images, i.e. $\Delta\phi(x, y) = \phi(x, y) - \phi_0(x, y)$. For objects of large conductivity and low permeability, such as the copper disks of this study, the phase values, $\Delta\phi(x, y)$ approximately represent the conductivity of the metallic specimen. The images are therefore proportional-conductivity maps of the object **(**Griffiths 2001; KORJENEVSKY 2000).

In the supplementary material of (Darrer 2015a) we have analysed the resolution of the images generated by our imaging system. This was carried out by applying a Canny edge-detection algorithm to copper and aluminium disks between 15 and 150 mm diameter and all 2 mm thickness. We determined the resolution to be 'the least diameter of the disks that gave and edge-detected diameter distinguishable from disks of smaller size', and found it to be ~30 mm.

3 SINGLE AND DOUBLE FERROMAGNETIC ENCLOSURES

The first goal of our research was to determine whether the MIT system could penetrate inside a ferromagnetic enclosure to extract an image of its contents, thus overcoming the effect of Faraday screening. Firstly, we demonstrate the penetrating power of our imaging modality, by imaging a copper disk concealed inside a 0.2 mm thick, ferromagnetic plated-steel-enclosure. Extracted images were obtained of a 30 mm diameter by 2 mm thick copper disk, in three locations within an enclosure of dimensions 75 mm × 77 mm × 15 mm. The Helmholtz-driver-coils were supplied with a (215 ± 2) mA RMS alternating current, at 200 Hz, providing a magnetic flux density of (0.42 ± 0.02) mT RMS at the level of the sensor coils. This low frequency field allows it to penetrate the walls of the enclosure to obtain a clear enough image of the object inside. The resultant images are shown in figure 3. We therefore demonstrated that the copper disk emits a magnetic field that can be detected, by escaping the enclosure walls and making contact with the sensor-coils outside; therefore giving away its shape and position. Additionally, we demonstrated that our imaging system is sensitive enough to generate an image of the disk, from its magnetic signature, using a method of subtraction-of-phases of the full and empty enclosures.

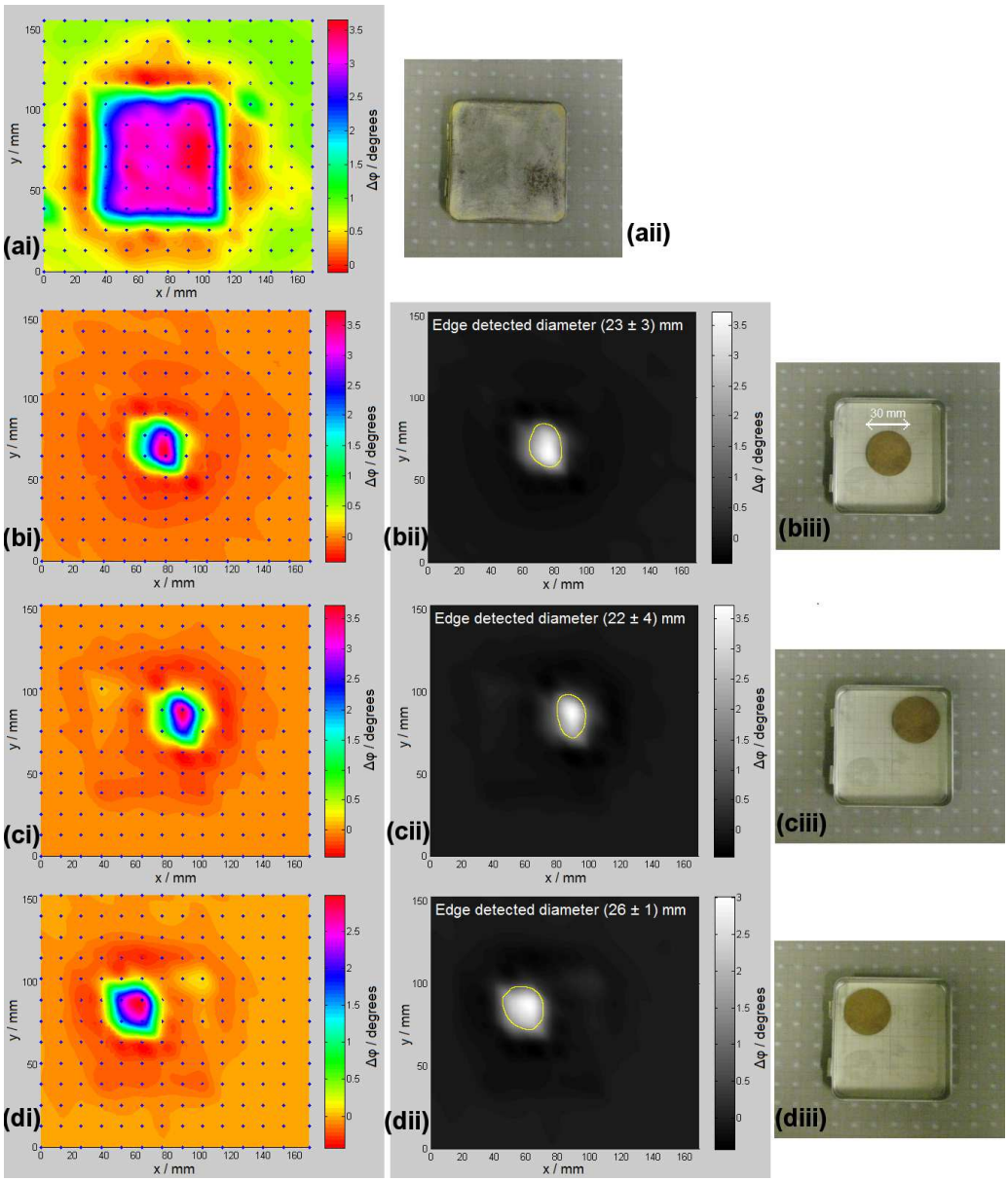

Figure 3. Extraction of copper disk-image from within a single ferromagnetic-enclosure. (ai) Magnetic image of empty closed-enclosure with photograph in (aii). The copper disk is 30 mm diameter by 2 mm thick. (bi) to d(i) show the extracted image of the disk in three positions, centre, upper right and upper left. (bii) to (dii) illustrates Canny edge-detection (see section 4) applied to the extracted images as a curved yellow line, approximately outlining the boundary of the disk. (biii) to (diii) are photographs of the disk inside the enclosure. The photographs show the enclosure lid removed, but images were captured with the lid on, concealing the disk.

A further demonstration of our magnetic-imaging system showed, that it could image a copper disk enclosed within a two-ferromagnetic-enclosure assembly. The copper disk was 40 mm diameter by 3 mm height. We used an identical magnetic-field and frequency of the previously described single enclosure, and the same image-penetration method of subtraction-of-phase-values of the full and empty enclosure images. The two plated mild-steel enclosures have the following dimensions. The smaller enclosure is, 88 mm × 89 mm × 9 mm, with material thickness (0.24 ± 0.01) mm; and the larger enclosure is 145 mm × 113 mm × 17 mm, with material thickness (0.33 ± 0.01) mm. The copper disk was placed in the smaller enclosure, which in turn was placed within the larger one. Magnetic images were taken of the concealed disk in three different positions, as shown in figure 4.

Figure 4(ai) shows a magnetic-image of the empty closed-double-enclosure with a photograph in figure 4(aii). Figures 4(bi) to 4(di), show the magnetic image of the enclosures with the disk concealed in the three positions of centre, left and right. It is not apparent on visual examination of

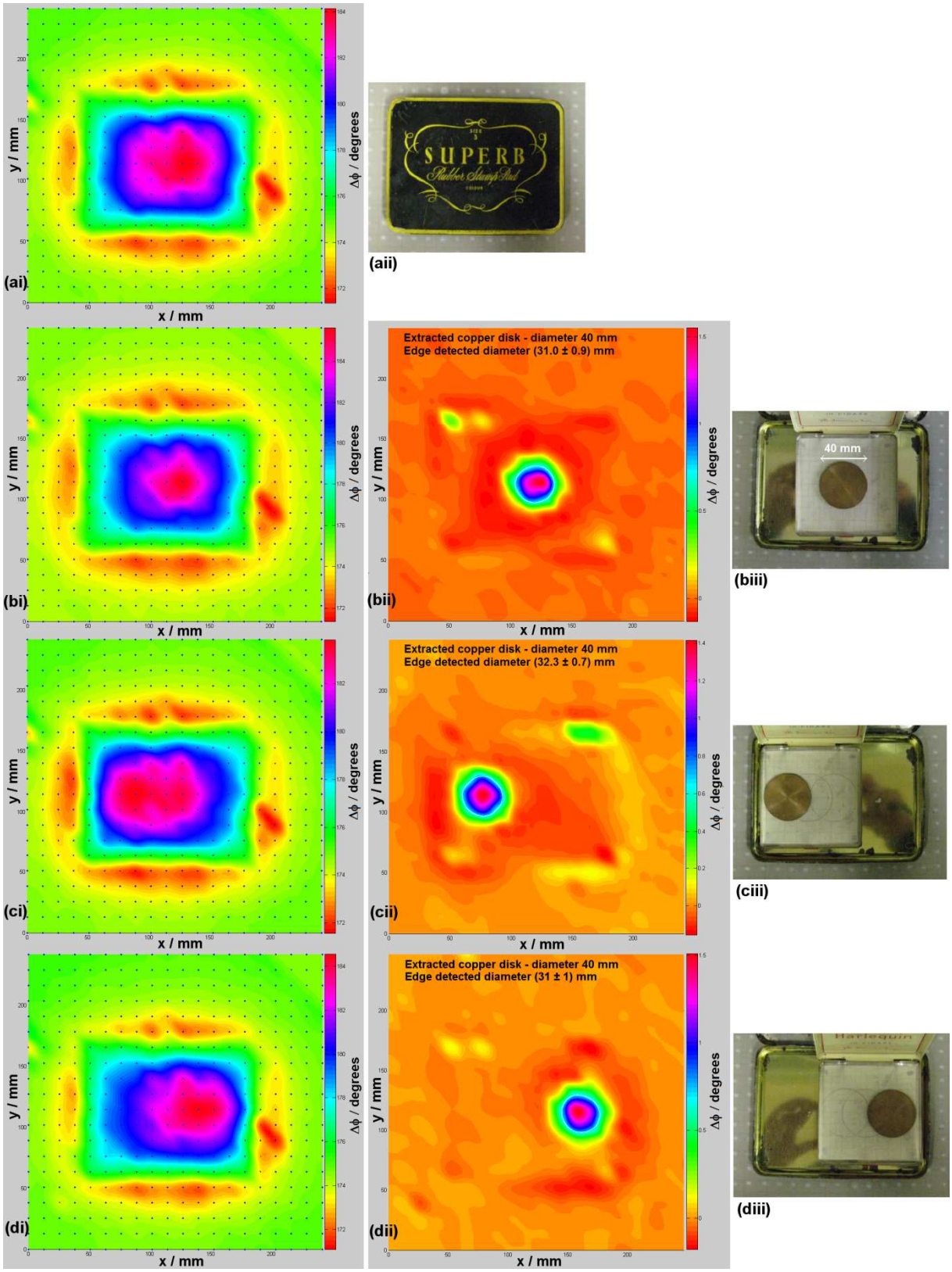

Figure 4. Illustration of magnetic imaging of a copper disk through a double ferromagnetic-enclosure. The copper disk is 40 mm diameter by 3 mm height. (ai) shows an image of the empty double-enclosure with photograph in (aii). (bi) to (di) shows magnetic image of the closed double-enclosure with concealed disk inside, in 3 positions of centre, left and right. (bii) to (dii) shows the extracted copper disk in the 3 positions, after subtraction of the empty enclosures' phases was applied to the full enclosures. (biii) to (diii) displays photographs of ferromagnetic double-enclosure with copper disk in the 3 positions. Photographs were taken with enclosure lids open, but magnetic images were taken with the enclosure lids closed.

these images, where the disk is located. The important result we describe here, is that a weak magnetic signature of the disk can be distinguished from the background of the total image, and that such a signature can be extracted to clearly show the disk's size and position. In figures 4(bii) to 4(dii) the method of subtraction-of-phases has been implemented, to clearly reveal the extracted copper disk. Firstly, an image is captured of the empty double-enclosure, then by carefully opening the enclosures, the disk is placed in the desired position. The enclosures are closed and a second image is taken of the full enclosure, followed by the subtraction-of-phases method for each sensor-coil position.

We have therefore demonstrated, firstly, that a weak magnetic signature of the copper disk contains enough information to construct an image of it, and secondly, that our imaging system is sensitive to such a signature.

4 DUAL FREQUENCY METHOD

It is obviously impractical in the real world to use the method of subtracting the empty enclosure from the full one; which only constitutes a proof-of-principle. To overcome this limitation we devised a new method that involves approximating the empty enclosure by using a higher frequency image, thereby removing the need to open the enclosure. At a sufficiently high frequency, penetration of the enclosure is reduced due to the skin effect (Wheeler 1942), allowing us to use this image in place of the empty enclosure. We demonstrated this technique, using a 30 mm diameter by 0.71 mm thick copper disk, concealed in a single plated-mild-steel-enclosure, of dimensions 145 mm × 113 mm × 17 mm, with material thickness (0.33 ± 0.01) mm, as the one described in section 3. Two images were taken of the enclosure containing the disk, one at low frequency, 200 Hz, and one at high frequency, 2 kHz. This procedure was repeated for the disk in three positions, centre, lower-right and upper-left. We have also included a 10 kHz image in figure 5(aii) in place of the 2 kHz image, to show the effect of increasing the frequency. In figure 5(ai) to 5(ci) the 200 Hz image is shown, with the disk in three positions. Figures 5(aii) to 5(cii) show the high frequency image, 10 kHz in 5(aii) and 2 kHz in 5(bii)-(cii). The low frequency image, $f_{low\ freq}(x, y)$, was normalised as, $f_{normalised}(x, y)$, to be the same order of phase values as the high frequency one, $f_{high\ freq}(x, y)$. In other words, at an arbitrary location, (x_{ref}, y_{ref}), away from the concealed disk the positional-phase value in the low frequency image coincided with the corresponding one in the high frequency image, therefore bringing about a rescaling effect, as shown in (1).

$$f_{normalised}(x,y) = f_{low\ freq}(x,y) \times \frac{f_{high\ freq}(x_{ref}, y_{ref})}{f_{low\ freq}(x_{ref}, y_{ref})} \quad . \tag{1}$$

With the high frequency image approximating the empty enclosure and the low frequency image rescaled to be of the same order, the method of subtraction-of-phase-values was implemented as in the proof-of-principle method, described above. The resultant images, revealing the extracted disk, are shown in figures 5(aiii) to (ciii). We have also applied a Canny-edge-detection algorithm (Canny 1983; Canny 1986; Deriche 1987) to these last figures, showing the edge of the disk traced out in a white curved line. Parts of the enclosure edge are also picked up by the Canny-edge-detector. The 10 kHz image used as the empty-enclosure-approximation in figure 5(aii) appears to reduce the edge of the enclosure in the resultant image in figure 5(aiii), more so than the 2 kHz images in figure 5(biii-ciii). It is possible, that the 10 kHz image approximates the empty enclosure better than the 2 kHz images.

If the location of the disk is chosen for (x_{ref}, y_{ref}), this will cancel the disk's positional-image when the high and low frequency images are subtracted. Therefore, a position for (x_{ref}, y_{ref}) away from the concealed disk is required. We found that the edge of the enclosure gave the best result. Although, this is not absolute, and (x_{ref}, y_{ref}) can vary a certain amount within the enclosure and still give a valid result, but not in the location of the disk. Therefore, as the MIT system stands at the moment, if the location of the disk is not known, there would need to be trial-and-error in establishing (x_{ref}, y_{ref}). From an initial first image, the edge can be determined, and then an edge chosen that is away from the disk, in order to image the object inside. For example, 2 or 3 edges could be tried, to see whether one of them revealed a concealed metallic object.

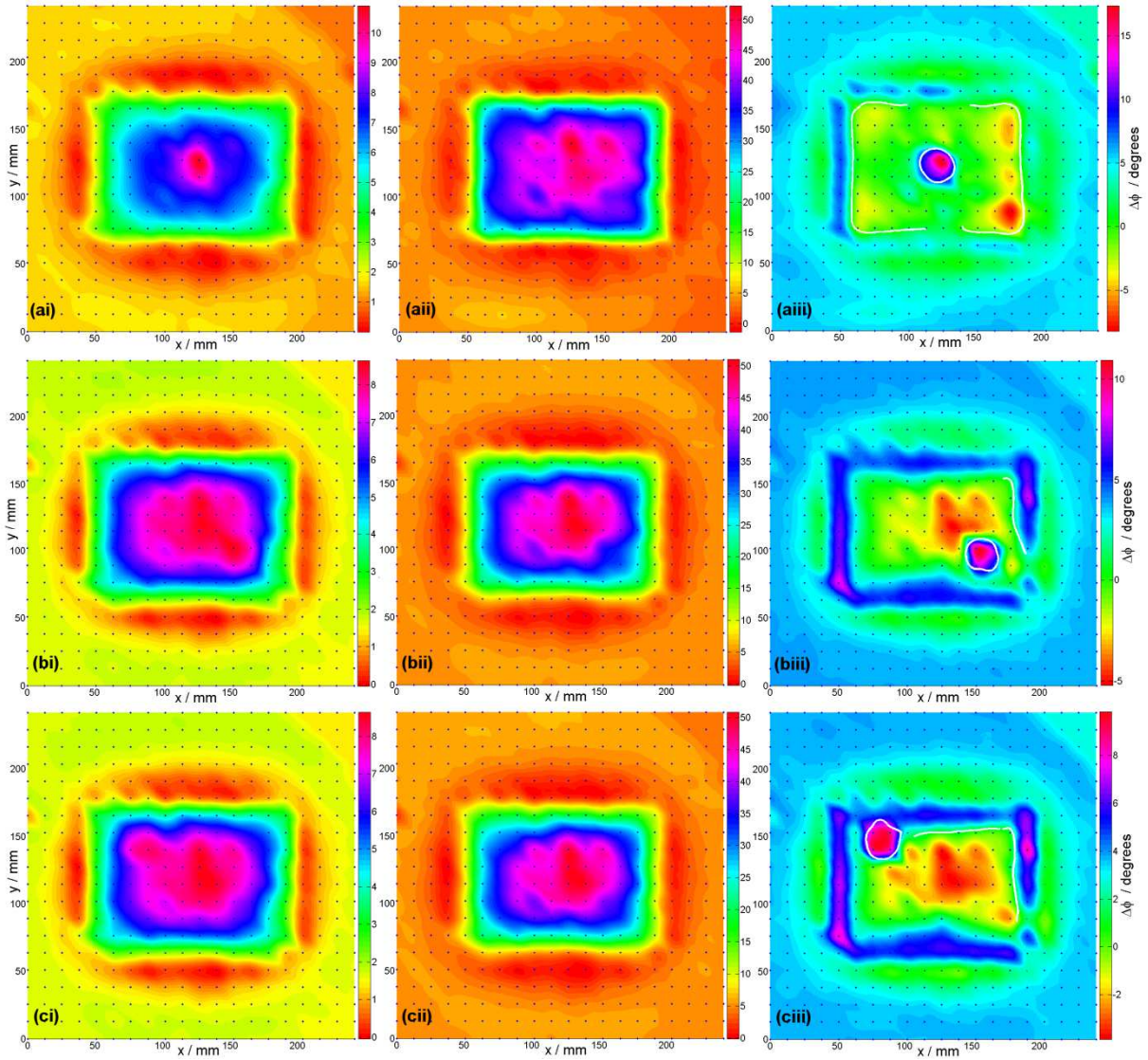

Figure 5. Magnetic images of a single ferromagnetic-enclosure, for extracting a copper disk using the dual-frequency method. (ai) to (ci) show the low frequency images at 200 Hz of the enclosure, with the disk in 3 positions of, centre, lower right and upper left. (aii) to (cii) displays the corresponding high frequency images at 10 kHz in (aii) and 2 kHz in (bii) to (cii). (aiii) to (ciii) displays the resultant images of the extracted copper disk, of 30 mm diameter by 0.71 mm height, in the 3 positions. The last column showing the resultant extracted images, (aiii - ciii), also illustrates Canny edge-detection, outlining the copper disk and parts of the enclosure edges, in a white curved line.

5 CONCLUSION

We have demonstrated that by using an electromagnetic-induction technique, it is possible to penetrate ferromagnetic enclosures to image the metallic contents inside. We have shown that the concealed objects have magnetic signatures that can pass through the metal walls of the enclosure and be detected by sensor-coils. By using an arrangement of array-based sensor-coils, it has been possible image inside the enclosures, revealing the position and shape of a concealed copper disk. We demonstrated that a weak magnetic signature can be detected from within a double-ferromagnetic enclosure, by subtracting the empty-enclosure phase values from the full enclosure. A practical technique was also invented that enables real-world applications of our MIT system. In the real world it is not practical to open a container and remove its contents, as we do with the proof-of-principle method. Our real-world technique requires a high frequency image to approximate the empty enclosure and a low frequency image to penetrate deeper into it, detecting the concealed contents. The main development here is that the principle of imaging inside a metallic enclosure, without removing its contents, using an ad hoc MIT method, has been demonstrated. The problem of the identification of an automatic process, and relative algorithm, to extract an image of the concealed object from the measurements, is currently an object of research in our group. We anticipate that it

may be possible to determine the material-type of the concealed object, from its magnetic signature, with the appropriate reconstruction algorithm. Our demonstration of the ability to image, and with the possibility of identifying materials through multiple layers of ferromagnetic-metallic-enclosures; makes this technique a potential image-scanning technology for the security industry.

6 ACKNOWLEDGMENT

This research was jointly funded by the Home Office and the Ministry of Defence, in the United Kingdom, and was commissioned by AWE.

7 REFERENCES

CANNY J.F., (1983), Finding edges and lines in images, *M.I.T. Artif. Intell. Lab.*, Cambridge, MA, TR-720

CANNY J.F., (1986), A Computational Approach to Edge Detection. *IEEE Trans. Pattern Anal. Mach. Intell*., 8, 679-698

DARRER B.J., WATSON, J.C., BARTLETT, P. RENZONI, F., (2015a), Magnetic imaging: a new tool for UK national nuclear security, *Sci. Rep*., 5 7944

DARRER B.J., WATSON, J.C., BARTLETT, P. RENZONI, F., (2015b), Toward an Automated Setup for Magnetic Induction Tomography, *IEEE Trans. Magn.*, 51(1) 6500104

DERICHE R., (1987), Using Canny's Criteria to Derive a Recursively Implemented Optimal Edge Detector, *Int. J. Comput. Vision*, 1, 167-187

GRIFFITHS H., (2001), Magnetic induction tomography, *Meas. Sci. Technol.*, 12, 1126-1131

GRIFFITHS H., GOUGH W., SWATSON S., AND WILLIAMS R.J., (2007), Residual capacitive coupling and the measurement of permittivity in magnetic induction tomography, *Physiol. Meas.*, 28 S301–S311

KORJENEVSKY A.V., CHEREPENIN V.A., SAPETSKY S., (2000), Magnetic induction tomography: experimental realization, *Physiol. Meas*., 21, 89-91

MA L., WEI, H-Y., SOLEIMANI, M., (2013), Planar magnetic induction tomography for 3D near subsurface imaging, *Prog. Electromagn. Res*., 138 65-82

MA X., PEYTON A.J., SOLEIMANI M., AND LIONHEART W.R.B., (2006), Imaging internal structure with electromagnetic induction tomography. In: *Instrumentation and Measurement Technology Conference, 24/27 April 2006, Sorrento*. IMTC 2006: Proceedings of the IEEE, 300

SOLEIMANI M., (2009), Simultaneous reconstruction of permeability and conductivity in magnetic induction tomography, *J. of Electromagn. Waves and Appl*., 23 785

WHEELER, H.A., (1942), Formulas for the Skin Effect, *Proc. IRE*, 30(9) 415